OXFORD Toxicology Research

Toxicology Research, 2021, **10**, 761–770

https://doi.org/10.1093/toxres/tfab060
Advance Access Publication Date: 29 June 2021
Paper

PAPER

Comparative effects of combined use of alcohol with cannabis and tobacco on testicular function in rats

Charles Obiora Nwonuma,[1,*] Osarenkhoe Omorefosa Osemwegie,[2] Emenike Onyebum Irokanulo,[2] Omokolade Oluwaseyi Alejolowo,[1] Omowumi Titilola Kayode,[1] Tomilola Debby Olaolu,[1] Adakole Sylvanus Ada,[3] Damilare Emmanuel Rotimi,[1] Roltdelmwa Filibus Maimako,[1] Adeyinka Samuel Adedayo[1] and Oluwafemi Adeleke Ojo[1]

[1]Department of Biochemistry, Landmark University, Omu-aran 370102, Nigeria, [2]Department of Microbiology, Landmark University, Omu-aran, Nigeria and [3]Department of Veterinary Physiology and Biochemistry, University Ilorin, Ilorin 240003, Nigeria

*Correspondence address. Department of Biochemistry, Landmark University, Omu-aran, Nigeria. E-mail: charlesdetermination@gmail.com

Abstract

Alcoholism has been linked to problems with male reproductive function. The combined effects of alcohol, cannabis, and tobacco were compared in this study. A total of 35 rats were assigned randomly into seven groups A–G: animals in A were administered distilled water. Animals in B–G were either administered alcohol orally (30 ml 40% alcohol) or exposed to smoke from ignited tobacco (exposure to smoke from 0.7 g tobacco for 5 min) or cannabis (exposure to smoke from 0.7 g tobacco and cannabis for 5 min): B (orally administered alcohol), C (exposed to the smoke from tobacco), D (exposed to smoke from cannabis), E (treated with alcohol and exposed to smoke from tobacco), F (treated with alcohol and exposed to smoke from cannabis), G (treated with alcohol and exposed to smokes from tobacco and cannabis). Assays were carried on the testicular homogenate after a 14-day treatment. There was a significant increase in activity of alkaline phosphatase ($P \leq 0.05$), concentrations of cholesterol, glutathione reductase, and malondialdehyde in treated rats by the co-administration of alcohol with cannabis and tobacco compared with the control group. The combined treatment also caused degeneration and morphological distortions of testicular cells. The biochemical and histoarchitectural change was due to oxidative damage attributable to the synergistic effects. The high binding energy of tetrahydrocannabinol ligand to prostate acid phosphatase may be a prediction that the ligand can have an inhibitory effect on the function of enzymes in the prostate.

Key words: alcohol, cannabis, oxidative stress, histopathology, testicular functions, tobacco

Introduction

Some lifestyles have been found to influence sperm production in humans and can cause biochemical changes that affect endocrine function, antioxidant status, and the morphological or fertilizing ability of male sex cells [1]. The altered morphology and defective sperm function have been linked to reactive oxygen species, according to research. [2]. Nicotine, a bioactive principle in tobacco has been reported to adversely affect spermatogenesis and lead to cellular depletion by suppressing the testosterone biosynthesis, reducing messenger RNA (mRNA) and protein levels of bcl-2, and upregulating the p53 and caspase-3 mRNA and protein levels [3]. Tobacco smoke also includes

Received: 3 April 2021; **Revised:** 24 May 2021; **Accepted:** 2 June 2021

harmful chemicals such as arsenic, hydrogen cyanide, lead, and benzene, some of which may be mutagens, aneugens, and carcinogens. Smoking has been shown in several studies to impair sperm motility and reduce the proportion of morphologically normal sperm. [4–6]. Previous researches in humans have also shown that smoking results in a secretory dysfunction of both Sertoli and Leydig cells [7]. The two elucidated cannabinoids are delta-9 tetrahydrocannabinol and cannabidiol [8]. In previous research, cannabinoids or their derivatives were found to bind to endocannabinoid receptors, which are part of the endocannabinoid system. The dynamic effect of cannabinoids on binding to endocannabinoid receptors have been reported to play a strategic role in male reproductive function and other biological processes related to nervous system development, synaptic plasticity, as well as a general response to environmental insults [9]. Furthermore, alcohol has been shown to block the hypothalamus–pituitary–gonadal axis' feedback mechanisms, causing damage to the proteins required for spermatogenesis and a decline in blood levels of testosterone [10]. Long-term alcoholic and tobacco use can increase the risk of acquired infertility in many adult males by fragmenting the DNA of previously healthy sperm [11]. This research investigated the biochemical and histopathological changes in the rat testis caused by alcohol consumption, as well as the co-use with tobacco and cannabis. The structure of the enzyme–inhibitor complex was also investigated in this study, which involved computational docking of alcohol, cannabis, and tobacco ligands to the active site of human prostate acid phosphatase.

Materials and Methods

Alcohol, tobacco, and cannabis

The National Drug Law Enforcement Agency provided cannabis leaf for this research, whereas Philip Morrison International British American Tobacco (Lisnafillan, Ballymena, Northern Ireland) provided tobacco leaf. Chelsea London Dry Gin provided the distilled alcohol (Lagos, Nigeria).

Preparation of alcohol/reagents

Fourteen milliliters of gin was dissolved in 6 ml of distilled water (v/v: 7/3). Each rat was given 0.2 ml of the mixture.

Animal grouping and treatment

A total of 35 rats with an average weight of 140 ± 0.5 g were purchased from the animal house of the Biochemistry Department, University of Ilorin Kwara State, Nigeria. The rats were acclimatized for 7 days, allowed access to food and water *ad libitum*. Ethical approval for the handling of the experimental animals was obtained from the University of Ilorin Ethical Committee (UERC/ASN/2017/902). The experimental animals were randomly distributed into seven groups: A, B, C, D, E, F, and G with five rats in each group. Group A (control) received 0.2 ml of distilled water via oral gavage. Similarly, each rat in groups B, E, F, and G was orally administered 30 ml of 40% alcoholic per volume (0.14 ml of the alcohol was administered in 0.06 ml of water as a vehicle). Subsequently, rats in groups C, E, and G were independently exposed to smoke from burnt 0.7 g of tobacco each. In a ventilated chamber measuring 50 × 50 × 50 cm^3, tobacco was suspended and ignited. The rats were placed in the compartments of the chamber for 5 min to inhale the trapped tobacco smoke. The rats in groups D, F, and G inhaled smoke from 0.7 g of cannabis in the chamber for 5 min. The animals were euthanized 24 h after the last treatment of the 14-day experiment. The testes were collected and homogenized in an appropriate buffer for a specific biochemical assay. A section of the testis was preserved for histopathological examination.

Biochemical analyses

Biochemical parameters were estimated in the testicular sample homogenate using a digital UV/visible spectrophotometer (Jenway, England).

Organ–body weight ratio. The organ–body weight ratio is the organ weight to the total body weight [12]: organ weight/total body weight × 100.

Total protein concentration. Protein concentration was evaluated using the method described by Gornall *et al*. [13]. Four milliliters of biuret reagent was added to 1 ml of sample homogenate; 1 ml of sample homogenate was mixed with 4 ml of biuret reagent. The mixture was left to sit for 30 min before being measured at 340 nm. The protein concentration was determined as follow: *Cs* × *F* (mg/ml), where *Cs* is the corresponding protein concentration from the standard curve and *F* is the dilution factor.

Determination of alkaline phosphatase (ALP) activity. The method used for this assay was described by Wright *et al*. [14]. The appropriately diluted sample was added to the mixture of 2.2 ml of 0.1 M carbonate buffer, 0.1 ml of 0.1 M $MgSO_4.7H_2O$ and incubated at 37°C for 10 min; 0.5 ml of *P*-nitrophenyl phosphate (PNPP) (10 mM) was added to the preceding mixture and incubated at 37°C for 10 min. The reaction was terminated using 2 ml of 1 M NaOH and absorbance was measured at a wavelength of 400 nm. Activity (nM/min/mg protein) =; ΔOD/min = change in the optical density of the reaction mixture per minute; TV = total volume of the reaction mixture; *F* = total dilution factor; SV = volume of the appropriately diluted sample; *L* = light path length; 9.9 is the extinction coefficient of 1 µm of PNPP in the alkaline solution of 1 ml volume and 1 cm path length; 1000 is the dilution factor introduced, which can express the enzyme activity in nM/min/mg protein.

Determination of acid phosphatase (ACP) activity. The method used in this assay was described by Wright and Leathwood [15]. The appropriately diluted sample was added to the mixture of 2.2 ml of sodium acetate buffer and incubated at 37°C for 10 min; 0.5 ml of PNPP (10 mM) was added to the preceding mixture and incubated at 37°C for 10 min. The reaction was terminated using 2 ml of 1 M NaOH and the absorbance was taken at a wavelength of 400 nm. Enzyme activity (nM/min/ml) =; Where: ΔOD/min = Change in optical density of reaction mixture per minute; SV = Volume of enzyme soutrce; L = Light path length (1cm); TV = Total volume of the reaction mixture; F = Total dilution factor; 9.9 = Extinction co-efficient of 1µm of p-nitrophenol in an alkaline solution of 1 ml volume and 1cm path length; 1000 = The factor introduced to enable the enzyme activity to be expressed in nM/min/mg protein.

Determination of superoxide dismutase (SOD) activity. The method described by Misra and Fridovich [16] was used to estimate superoxide dismutase activity; 0.3 ml of 0.3 mM adrenalin was added to 2.5 ml 0.001 M phosphate buffer (pH 1.02); and 0.2 ml of water

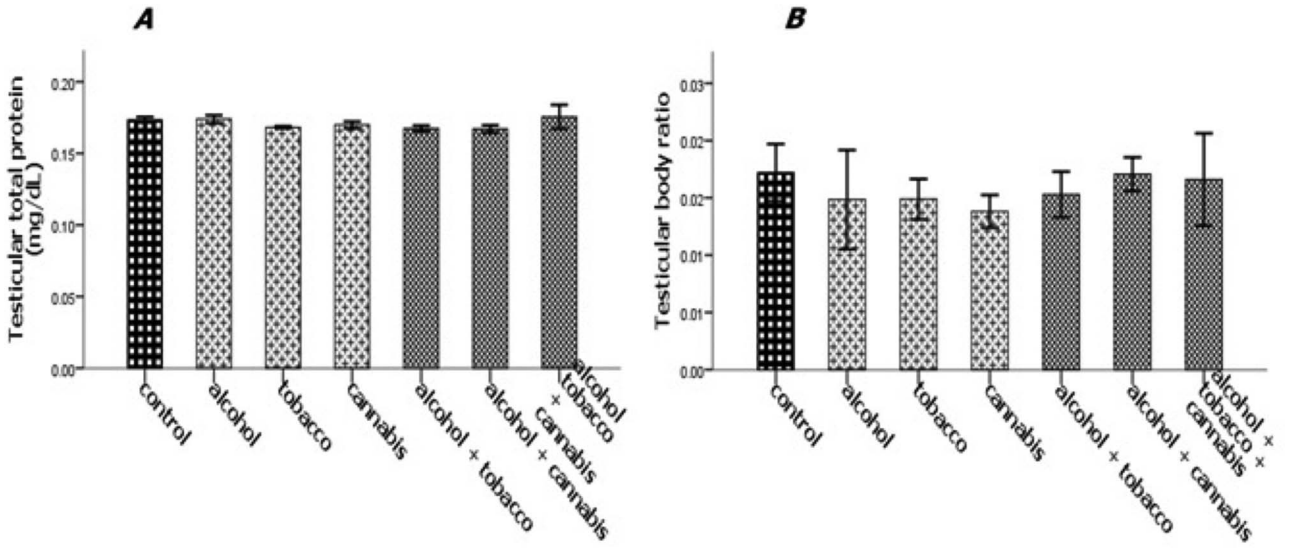

Figure 1: Effect of alcohol and co-administration with tobacco and cannabis on the testicular–body ratio (**A**) and testicular total protein (**B**) of male rats. Mean ± SEM of four variables. At $P < 0.05$, the bars with different superscripts are significantly different.

was added to the mixture and vortexed to obtain a homogeneous mixture. The increase in absorbance at 480 nm was monitored every 30 s for 150 s. Calculation: increase in absorbance (per min) =; A0 = absorbance after 30 s, A3 = absorbance after 150 s. Percentage of inhibition =

$$\frac{\text{increase in absorbance of the substrate}}{\text{increase in absorbance of blank}} \times 100$$

Determination of catalase activity. Catalase activity was measured by the method described by Beers and Sizer [17]; 0.1 ml of appropriately diluted sample was added to a cuvette containing 1.9 ml of 50 mM phosphate buffer (pH 7.0) and reaction was started by the addition of 1.0 ml of freshly prepared 30 mM H_2O_2. The rate of decomposition of H_2O_2 was measured spectrophotometrically from changes in absorbance at 240 nm. The activity of catalase was measured in units/mg protein.

Determination of reduced glutathione. The level of reduced glutathione was assayed according to Jollow *et al.* [18]. An aliquot (0.5 ml) of the homogenate was deproteinized by the addition of an equal volume of 4% sulfo-salicylic acid and then centrifuged at 3000 rpm for 15 min at 20°C; 0.5 ml of the supernatant was then added to the 4.5 ml Ellman reagent. A blank was prepared with 0.5 ml of sulfo-salicylic acid in 0.1 M phosphate buffer (twice dilution) and 4.5 ml of Ellman reagent. The absorbance was read within 5 min of the generation of yellow color on the addition of Ellman reagent at 412 nm.

Determination of lipid peroxidation. The sample lipid peroxidation was estimated according to the method described by Kei [19]. Thiobarbituric acid reactive substance was measured as an estimate of malondialdehyde (MDA), which is a product of lipid peroxidation. 1.6 ml of 30% trichloroacetic acid was added to .4 ml of appropriately diluted sample and vortexed; 0.5 ml of 0.050% thiobarbituric acid was added to the mixture and vortexed. The reaction mixture was heated at 45 min at 80°C for color development. This was again cooled in ice after heating for 10 min. After shaking vigorously, this was centrifuged at 5000 rpm for 10 min. The absorbance of the supernatant, which is the organic phase, was then taken at 532 nm.

Indirect assessment of HMG-CoA/mevalonate ratio. β-Hydroxyl-β-methylglutaryl coenzyme A (HMG-CoA) reductase was also estimated according to Rao and Ramakrishnan [20] by measuring the concentration of HMG-CoA and mevalonate. The ratio of HMG-CoA to mevalonate is taken as a measure of HMG-CoA reductase activity; 10% of the fresh tissue homogenate was mixed with an equal volume of dilute perchloric acid (50 ml/l). The mixture was allowed to stand for 5 min and centrifuged (2000 rpm 10 min). One milliliter of the filtrate was added to 0.5 ml of freshly prepared hydroxylamine reagent (alkaline hydroxylamine reagent in the case of HMG-CoA) mix, and after 5 min, 1.5 ml of ferric chloride reagent is added to the same tube and shake well. After 10 min, the sample absorbance was taken at 540 nm vs a similarly treated saline/arsenate blank.

Lipid extraction and profiling of the testes. The method for the extraction of lipid from tissue sample was described by Folch *et al.* [21]; 10% of testicular homogenate was prepared by homogenizing 0.2 g of the tissue in 0.8 ml of chloroform/methanol (2:1; v/v) using Teflon homogenizer at 4°C. The homogenate was then centrifuged at 5000 rpm at 4°C, after which the chloroform portion of the mixture (supernatant) was taken. The chloroform extract was subsequently washed in 0.1 ml of 0.05 M KCl solution, after which the mixture was centrifuged again and the chloroform (lower layer) was removed for lipid profiling. The method described by Allain *et al.* [22] was used to estimate cholesterol concentration in the sample; 100 µl of the lipid extract was evaporated to dryness at 60°C; 20 µl of Triton-X/chloroform mixture was added and vortexed and evaporated to dryness. One milliliter of cholesterol reagent was incubated for 20 min, and the absorbance was taken at 550 nm within 30 min against the reagent blank. Similarly, the triglyceride concentration in each sample was quantified by the method described by Kriketos *et al.* [23]. One hundred microliters of the extract was evaporated to dryness. After cooling, 100 µl of

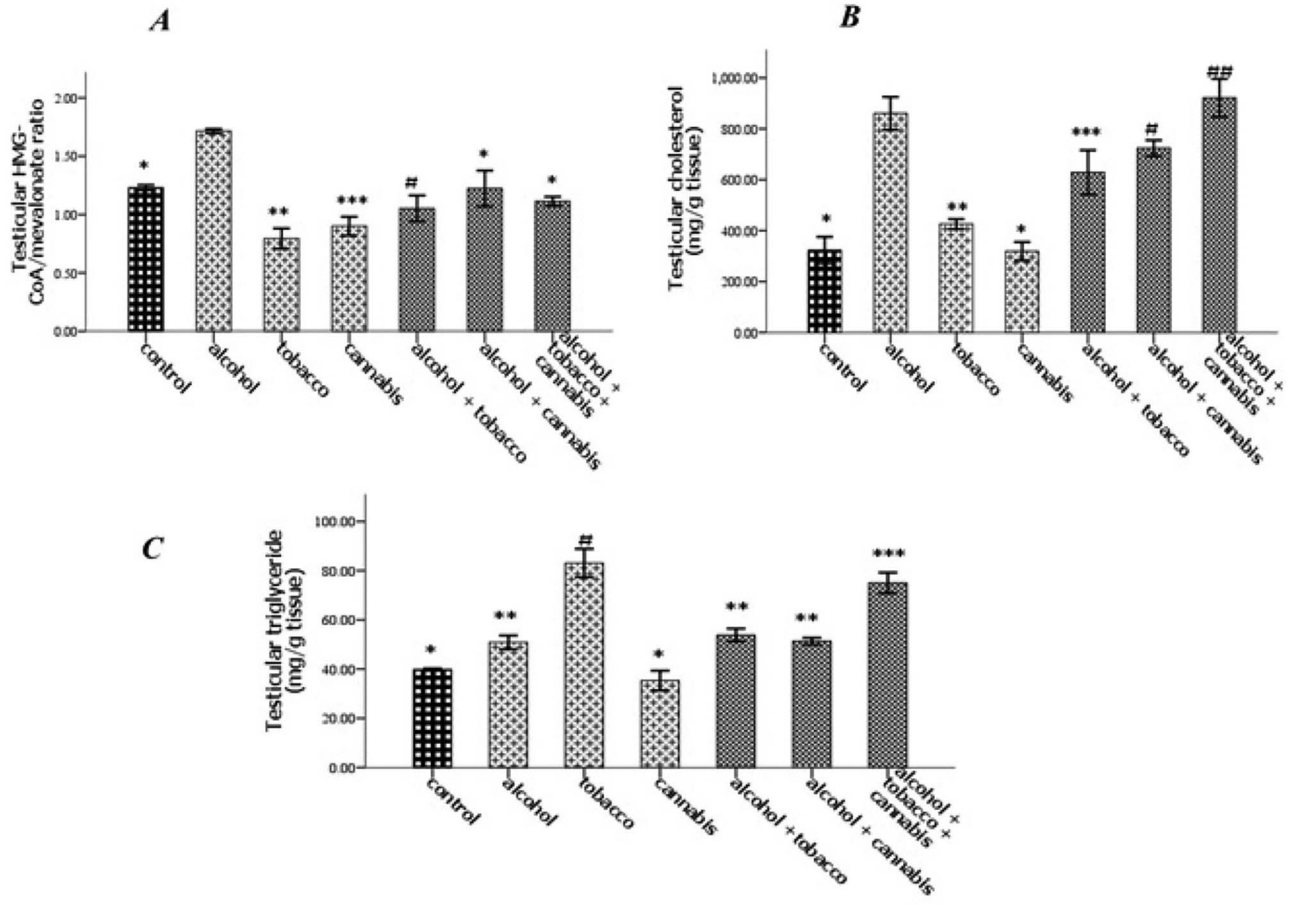

Figure 2: Effect of alcohol and co-administration with tobacco and cannabis on the testicular HMG-CoA and mevalonate ratio (**A**), testicular cholesterol concentration (**B**), and testicular triglyceride concentration (**C**) in rats. Mean ± SEM of four variables. At $P < 0.05$, the bars with different superscripts are significantly different.

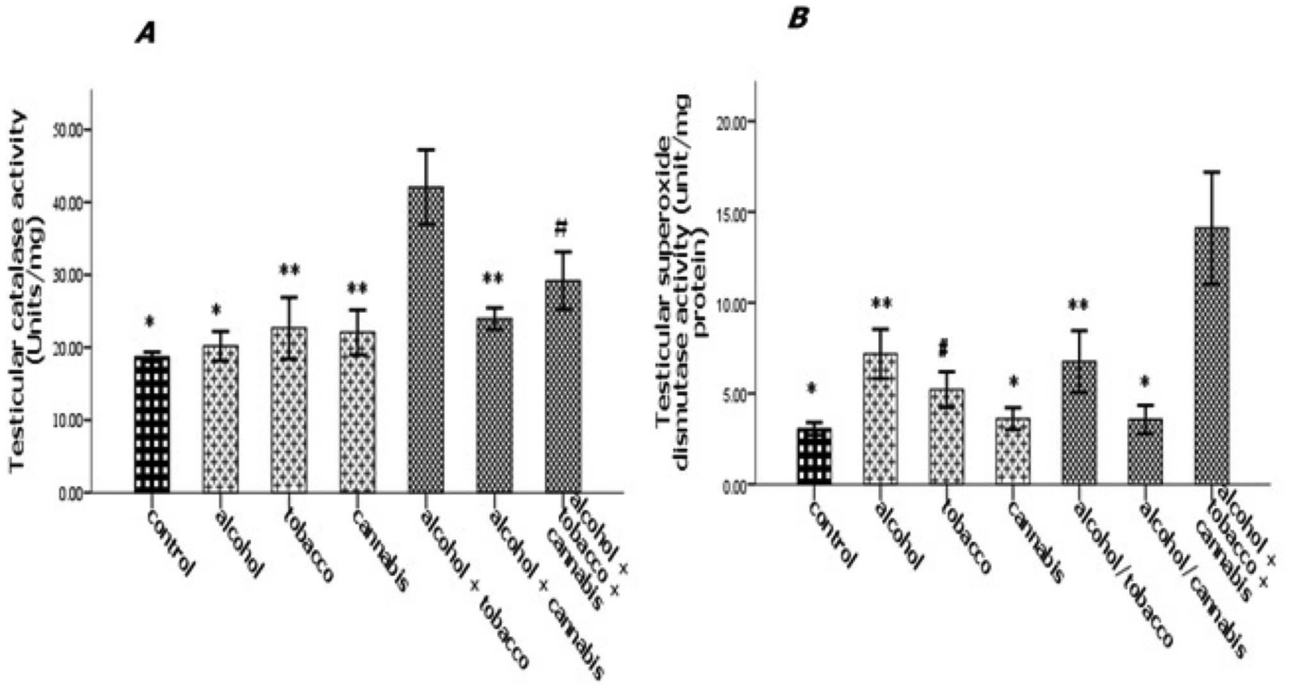

Figure 3: Effect of alcohol and co-administration with tobacco and cannabis on the testicular catalase activity (**A**) and testicular superoxide dismutase activity (**B**) in rats. Mean ± SEM of four variables. At $P < 0.05$, the bars with different superscripts are significantly different.

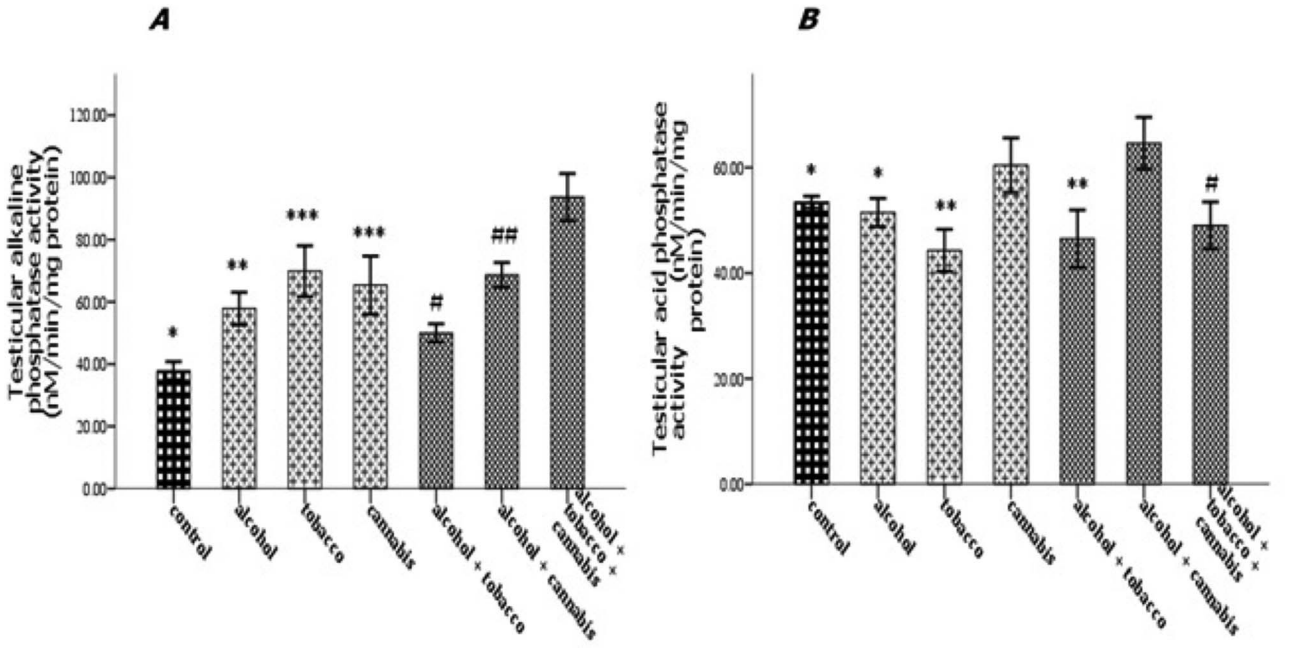

Figure 4: Effect of alcohol and co-administration with tobacco and cannabis on the testicular alkaline phosphatase activity (**A**) and testicular acid phosphatase activity (**B**) in rats. Mean ± SEM of four variables. At $P < 0.05$, the bars with different superscripts are significantly different.

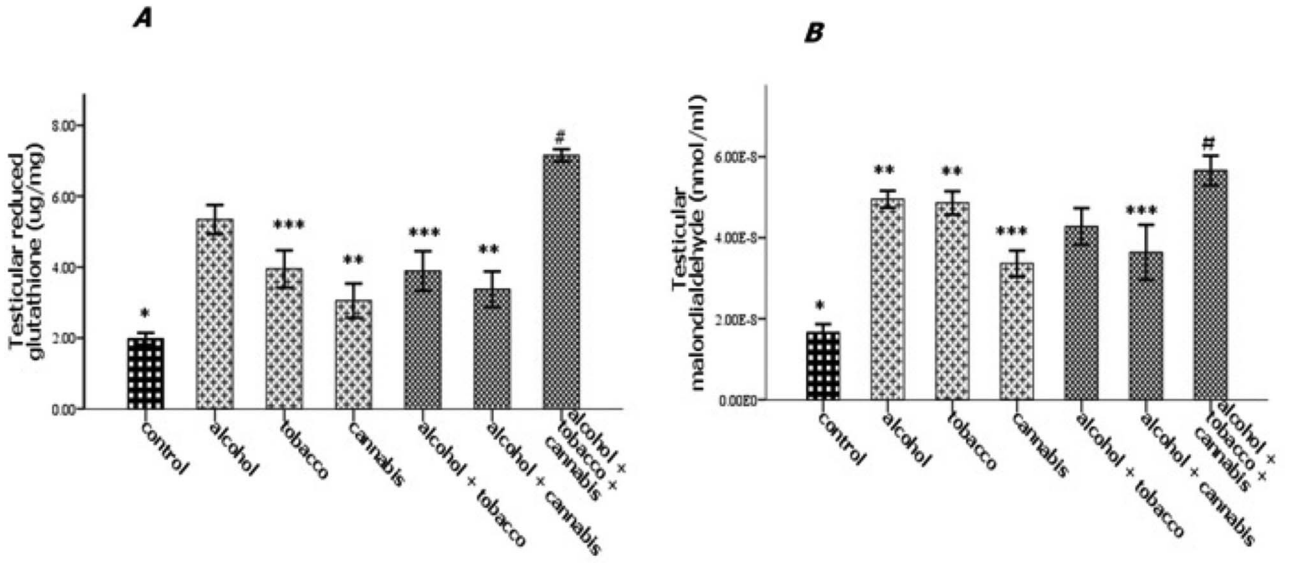

Figure 5: Effect of alcohol and co-administration with tobacco and cannabis on the testicular glutathione reductase concentration (**A**) and malondialdehyde (**B**) in rats. Mean ± SEM of four variables. At $P < 0.05$, the bars with different superscripts are significantly different.

97% of ethanol was added to the dried extract. One milliliter of triglyceride reagent was added and incubated for 20 min, and the absorbance of the sample and standard were measured within 30 min at 505 nm against the reagent blank.

Histopathology

Tissue samples of the testis from the rats were fixed in formaldehyde (10%, v/v). The histology tissue preparation was done using the method described by Hewitson and Darby [24]; the tissue samples were trimmed for microtomy. The trimmed blocks were sectioned at 7 µm thickness. The tissue ribbon was picked on a glass slide, dried, and stained in hematoxylin and eosin (H&E) stains. Slides were captured by a camera attached to the microscope and then analyzed for histopathology. The H&E stains coupled with the microscopic tissue analysis was done using the method described by Cardiff *et al.* [25]

Molecular docking method

The following chemical ligands: nicotine, alcohol, and tetrahydrocannabinol were docked to crystal structures of human prostatic acid phosphatase using Vina with AutoDock tools

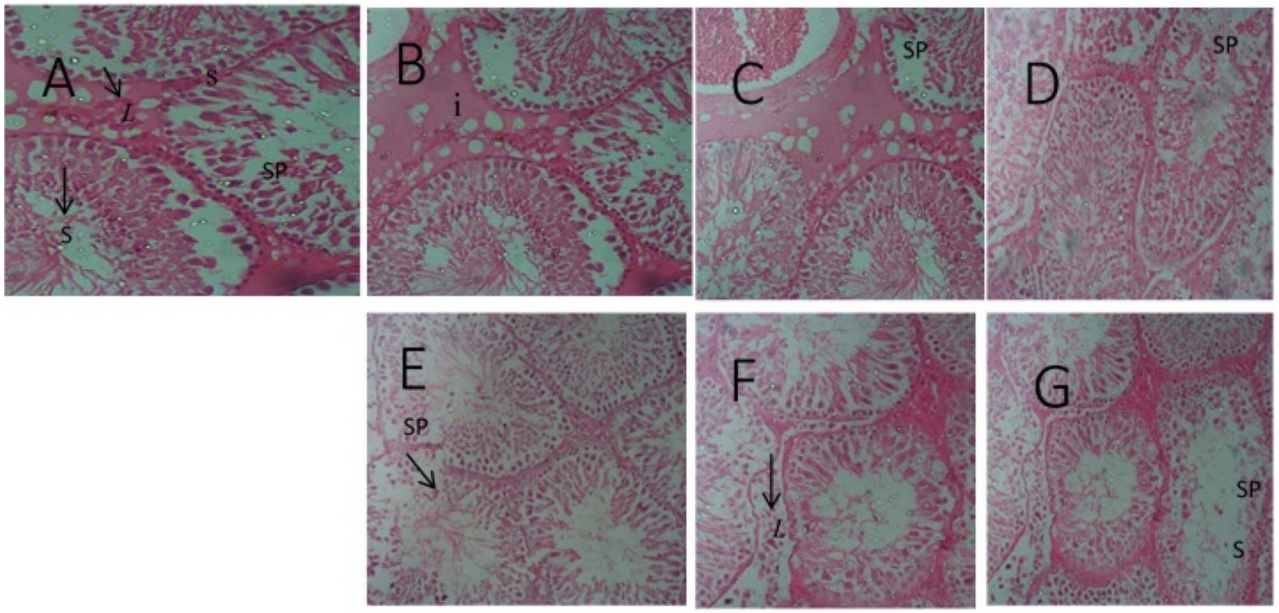

Figure 6: Testicular micrograph (H&E ×100): **(A)** Control; normal spermatogenic cells (SP), and no degeneration; **(B)** Alcohol; cells were normal with slight cell degeneration; **(C)** Tobacco cell were abnormal and degenerated; **(D)** Cannabis; normal cells and slightly abnormal cells; **(E)** Alcohol and Tobacco; morphological distorted cell and germinal cell degeneration; **(F)** Alcohol and Cannabis; cell morphological distortion and cell apoptosis; **(G)** Alcohol, Tobacco, and Cannabis; spermatogenic cells apoptosis and cells morphological distortion. Leydigs cell (L), seminiferous tubules (S).

and PyMol [26]. A subunit of the complex protein prostate acid prostate acid phosphatase (PAP) (PDB code: IND5) was used in the study, which also offers insight into inhibitor design.

Statistical evaluation

Values were expressed as the mean ± SEM of four animals per group. One-way analysis of variance test followed by Tukey *post hoc* multiple comparisons test was used to estimate significant differences among the variables. Values were considered statistically significant at $P < 0.05$. All the data were subjected to statistical analysis using IBM SPSS (Statistical Package for Social Science) statistic 23 (SPSS Inc., Chicago, IL, USA).

Result

The experimental rats across the treatment groups did not show any significant ($P > 0.05$) change in the testicular–body ratio compared with the rats in the control group (Fig. 1A). Similarly, the testicular protein concentration did not show a significant ($P < 0.05$) change in rats across treatment groups compared with the rats in the control group (Fig. 1B). Animals administered alcohol alone showed a significant ($P < 0.05$) increase in the HMG-CoA–mevalonate ratio compared with the animals in the control group. However, the HMG-CoA–mevalonate ratio decreased significantly ($P < 0.05$) in rats exposed to other treatments when compared with the control group. Only the animal exposed to cannabis smoke showed an exception to this trend (Fig. 2A). Similarly, testicular cholesterol and triglyceride levels significantly ($P < 0.05$) increased in rats across treatment groups compared with the rats in control groups, except for the rats that were exposed to cannabis smoke (Fig. 2B and C). Also, there was a significant ($P < 0.05$) increase in catalase activity in rats across the treatment groups compared with the rats in the control group, except in the rats administered alcohol (Fig. 3A). Superoxide dismutase activity in rats in groups B, C, E, and G, respectively, showed a significant ($P < 0.05$) increase (Fig. 3B). Alkaline phosphatase (ALP) activity increases significantly ($P < 0.05$) in rats across the treatment groups, with the highest increase observed in group G (Fig. 4A). Furthermore, a significant ($P < 0.05$) decrease was observed in the ACP activity of rats in groups C, E, and G, respectively, but there was a significant increase in rats in groups D and F compared with animals in the control group (Fig. 4B). Also, there was a significant ($P < 0.05$) increase in reduced glutathione concentration across rats in the treatment groups compared with the rats in control groups; however, there was a pronounced increase in rats given only alcohol, tobacco, and cannabis, respectively (Fig. 5A). Similarly, there was a significant ($P < 0.05$) increase in MDA in rats across the treatment groups though with varying degrees of lipid peroxidation, which also was dependent on the administered substances and the manner of administration (Fig. 5B). Testicular histology showed cellular degeneration across all the treatments, but with obvious effect in the groups treated with alcohol, tobacco, and alcohol jointly with tobacco when compared with the rats in control groups. Conversely, the rats exposed to the smoke from cannabis alone showed slightly normal testicular cell integrity compared with the animals in the control groups (Fig. 6). The negative binding energy of tetrahydrocannabinol ligands between amino acid residues in the active sites of prostate acid phosphatase was higher (−7.0 kcal/mol) compared with nicotine and alcohol (Fig. 7). The binding free energies of alcohol, nicotine, and tetrahydrocannabinol are −2.6, −5.8, and − 7.0 kcal/mol, respectively (Table 1). Tetrahydrocannabinol complied with the Lipinski rules compared with nicotine and alcohol (Table 2). The compound also complied with the ADMET (absorption, distribution, metabolism, excretion, and toxicity) drug properties (Table 3).

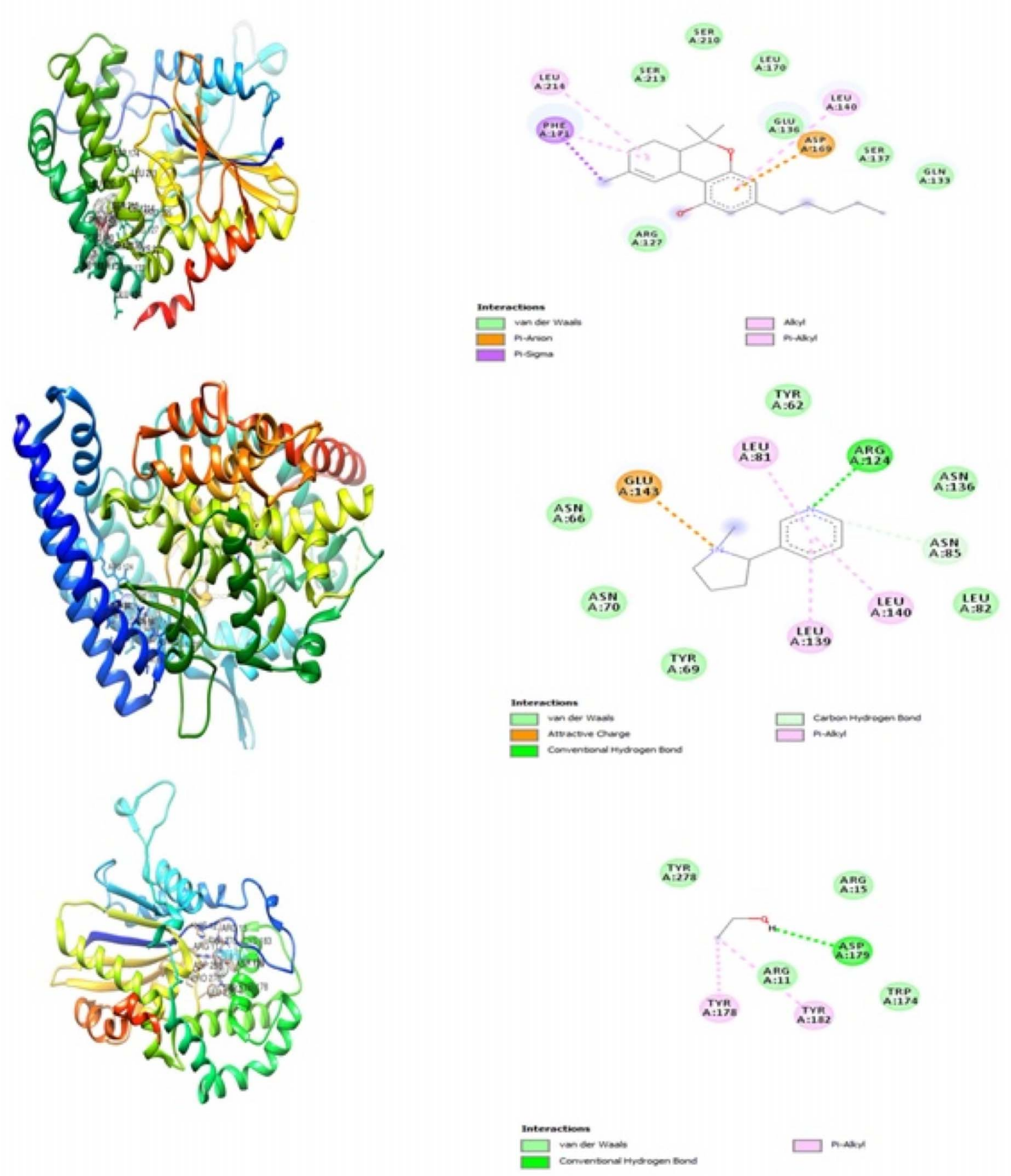

Figure 7: The interacting modes of tetrahydrocannabinol showing the 3D and 2D structures, respectively: (1a and 2a), nicotine (1b and 2b), and alcohol (1c and 2c) with the adjacent amino acid residues in the active site of human prostatic acid phosphatase.

Table 1: Binding energy in kcal/mol of tetrahydrocannabinol, nicotine, and alcohol with prostate acid phosphatase

Compounds	Docking score (kcal/mol)
Tetrahydrocannabinol	−7.0
Nicotine	−5.8
Alcohol	−2.8

Discussion

The insignificant reduction in testicular–body ratio observed in experimental rats in this study may suggest progressive cell death or morphological changes. The total protein concentration in the testes of rats given alcohol, tobacco, or cannabis was unaffected, suggesting that sperm cell testicular protein synthesis was unaffected. Protein synthesis is vital for spermatogonial stem cell regeneration, sperm maturation, and pattern formation

Table 2: Oral drug-likeness of the tetrahydrocannabinol, nicotine, and alcohol using Lipinski rule of five filters

Compound	Molecular weight (Dalton)	Log *P*	Number of HBD	Number of HBA	Molar refractivity	Number of rotatable bonds
Tetrahydrocannabinol	314.46	1.7903	1	2	97.91	4
Nicotine	162.23	1.2663	0	2	53.13	1
Alcohol	46.07	1.3617	1	1	12.89	0

HBD, hydrogen bond donor; HBA, hydrogen bond acceptor.

Table 3: ADMET properties of the tetrahydrocannabinol, nicotine, and alcohol predicted from admetSAR

ADMET	Tetrahydrocannabinol	Nicotine	Alcohol
BBB	Yes	Yes	No
GI absorption	High	High	No
Ames toxicity	No	No	No
Carcinogenicity	No	No	No
Pgp	No	No	No
CYP 2C19 inhibitor	Yes	No	No
CYP 2C9 inhibitor	Yes	No	No
CYP 1A2 inhibitor	No	No	No
CYP 2D6 inhibitor	Yes	No	No
CYP 3A4 inhibitor	No	No	No
Skin permeation	−3.27 cm/s	−6.46 cm/s	−6.64 cm/s

BBB, blood brain barrier; CYP, cytochrome; GI absorption, gastrointestinal absorption; Pgp, permeability glycoprotein.

in transcriptional dynamics [27]. In the seminiferous tubules, the Sertoli cells also secrete proteins needed for testicular function [28]. In addition to being an integral part of the sperm cell membrane, lipids have been reported to contribute to the development of gonad hormones, sperm cell maturation, viability, and the ability of spermatozoa to penetrate egg cells during fertilization. [29]. However, previous research has found that plasma testosterone levels are inversely related to plasma cholesterol and triglyceride levels. According to the findings of this study, alcohol and tobacco use increased testicular cholesterol and triglyceride levels, which could be linked to testicular dysfunction [30, 31]. Ramirez *et al.* [32] also documented a high incidence of cholesterolemia and tryglyceridemia in a group of 100 infertile men [33, 34]. Furthermore, Kim *et al.* [35] also reported that high serum levels of cholesterol and triglyceride could be linked to poor semen quality and that a change in lipid metabolism in the seminal plasma was related to infertility. Cannabis, on the other hand, did not cause an increase in cholesterol or triglycerides, implying that cannabis smoking did not alter the testicular lipid status, which is implicated in male reproductive dysfunction. According to this present study, the increase in cholesterol and triglycerides caused by combining cannabis with alcohol and tobacco was due to the effects of alcohol and tobacco. HMG-CoA reductase is the rate-limiting enzyme in the biosynthesis of cholesterol. HMG-CoA/mevalonate ratio activity rises in lockstep with HMG-CoA/mevalonate ratio activity. The current study discovered an increase in the enzyme activity, which may be indicative of increased cholesterol production, with possible resultant infertility due to lipidemia [36]. Contrary, cannabis and tobacco caused a decrease in the activity of the enzyme. Furthermore, antioxidant defense mechanisms, both enzymatic and nonenzymatic, are well expressed in the testes [37]. The increased SOD and catalase activity in this study may have been triggered to mop up free radicals or reactive oxygen species (ROS) generated by alcohol, tobacco, and cannabis, which are responsible for oxidative stress [38, 39]. Similarly, the rise in glutathione levels in this study was also a biochemical response to neutralize lipid peroxidation. MDA is produced as a result of lipid peroxidation in the cell membrane. MDA level is proportional to the lipid peroxidation in the plasma membrane. The elevated MDA levels across the treated groups gave credence to the increased in the activity of antioxidant enzymes [40, 41]. Acid phosphatase, a viable marker for prostate function, is also found in testicular germ cells and plays a role in spermatocyte maturation [42]. In this research, it was discovered that tobacco, as well as tobacco combined with alcohol and cannabis, reduces the activity of this enzyme. Furthermore, ALP is abundant in the cell membrane on the absorptive or secretion surfaces of cells and aids in spermatogenesis, intermediate carbohydrate metabolism, and testicular hormone synthesis [43]. ALP is a cellular damage biomarker linked to androgenic activity [44]. The increase in ALP activity caused by alcohol, as well as co-administration of alcohol with tobacco and cannabis, may be attributed to either *de novo* synthesis or leakage from the degradation of the testicular cell membrane structure. A cross-section of the experimental rats' testes revealed morphological distortion and cell death due to alcohol, tobacco, and/or their combined use, which matched the biochemical changes. Steroid activity in the endoplasmic reticulum and mitochondrion of the Leydig cell is affected by testicular cell distortions or death [45]. In rats given only cannabis, the histological cell structure was standard. This may indicate that the chemical compounds present in marijuana smoke are not cytotoxic to testicular cells. The high affinity of tetrahydrocannabinol for the active site of prostate acid phosphate suggests that it may be used to prevent prostate cancer, and it also suggests that cannabis smoking alone might not be harmful to testicular function [46] unless combined with alcohol. Tetrahydrocannabinol follows Lipinski's law, and the ADMET prediction indicates that it will be a safe drug candidate.

Conclusion

The findings of this study suggested that the rats' male reproductive system was responsive to the treatment protocols, implying that the use of the tested substances could alter

important male reproductive functions. It is also worth noting that testicular biochemical and histopathological changes caused by alcohol consumption and/or its combined use with tobacco and cannabis were mainly attributable to oxidative damage caused by alcohol consumption or tobacco smoking. Beyond biochemical alterations and observed histopathological evidence, this study has provided the foundation for further analysis of the underlying mechanism. Tetrahydrocannabinol inhibited PAP primarily through hydrophobic interactions and a network of hydrogen bonds, according to molecular docking. The compound's ability to inhibit PAP made it a possible drug design candidate.

Authors' Statement

The authors declare that this manuscript is original and is not been considered for publication elsewhere. Also, all authors declare no competing interest all through the compilation of the work.

Conflict of Interest

None declared.

References

1. McMillen IC, Robinson JS. Developmental origins of the metabolic syndrome: prediction, plasticity, and programming. *Physiol Rev* 2005;**2**:571–633.
2. Ray PF, Toure A, Metzler-Guillemain C *et al*. Genetic abnormalities leading to qualitative defects of sperm morphology or function. *Clin Genet* 2017;**2**:217–32.
3. Mosadegh M, Hasanzadeh S, Razi M. Nicotine-induced damages in testicular tissue of rats; evidences for bcl-2, p53 and caspase-3 expression. *Iran J Basic Med Sci* 2017;**2**:199.
4. Stillman RJ, Rosenberg MJ, Sachs BP. Smoking and reproduction. *Fertil Steril* 1986;**4**:545–66.
5. Sofikitis N, Miyagawa I, Dimitriadis D *et al*. Effects of smoking on testicular function, semen quality and sperm fertilizing capacity. *J Urol* 1995;**3**:1030–4.
6. Zavos PM, Correa JR, Karagounis CS *et al*. An electron microscope study of the axonemal ultrastructure in human spermatozoa from male smokers and nonsmokers. *Fertil Steril* 1998;**3**:430–4.
7. Sofikitis N, Miyagawa I, Dimitriadis D *et al*. Effects of smoking on testicular function, semen quality and sperm fertilizing capacity. *J Urol* 1995;**3**:1030–4.
8. Hindocha C, Freeman TP, Schafer G *et al*. Acute effects of delta-9-tetrahydrocannabinol, cannabidiol and their combination on facial emotion recognition: a randomised, double-blind, placebo-controlled study in cannabis users. *Eur Neuropsychopharmacol* 2015;**3**:325–34.
9. Fasano S, Meccariello R, Cobellis G *et al*. The endocannabinoid system: an ancient signaling involved in the control of male fertility. *Ann N Y Acad Sci* 2009;**1**:112–24.
10. Gaur DS, Talekar MS, Pathak VP. Alcohol intake and cigarette smoking: impact of two major lifestyle factors on male fertility. *Indian J Pathol Microbiol* 2010;**1**:35.
11. Anifandis G, Bounartzi T, Messini CI *et al*. The impact of cigarette smoking and alcohol consumption on sperm parameters and sperm DNA fragmentation (SDF) measured by Halosperm®. *Arch Gynecol Obstet* 2014;**4**:777–82.
12. Busari MB, Muhammad HL, Ogbadoyi EO *et al*. In vivo evaluation of antidiabetic properties of seed oil of Moringa oleifera Lam. *J Appl Life Sci Int* 2015;**1**:160–74.
13. Gornall AG, Bardawill CJ, David MM. Determination of protein concentration by the biuret method using bovine serum albumin as a standard. *J Biol Chem* 1949;**177**:751–66.
14. Wright PJ, Leathwood PD, Plummer DT. Enzymes in rat urine: alkaline phosphatase. *Enzymologia* 1972;**42**:317–27.
15. Wright PJ, Leathwood PD. Plummer DT enzymes in rat urine: acid phosphatase. *Enzymologia* 1972;**42**:317–27.
16. Misra HP, Fridovich I. The generation of superoxide radical during the autoxidation of hemoglobin. *J Biol Chem* 1972;**21**:6960–2.
17. Beers RF, Sizer IW. A spectrophotometric method for measuring the breakdown of hydrogen peroxide by catalase. *J Biol Chem* 1952;**1**:133–40.
18. Jollow DJ, Mitchell JR, Zampaglione NA, Gillette JR. Bromobenzene-induced liver necrosis. Protective role of glutathione and evidence for 3, 4-bromobenzene oxide as the hepatotoxic metabolite. *Pharmacology* 1974;**3**:151–69.
19. Kei S. Serum lipid peroxide in cerebrovascular disorders determined by a new colorimetric method. *Clin Chim Acta* 1978;**1**:37–43.
20. Rao AV, Ramakrishnan S. Indirect assessment of hydroxymethylglutaryl-CoA reductase (NADPH) activity in liver tissue. *Clin Chem* 1975;**10**:1523–5.
21. Folch J, Lees M, Stanley GS. A simple method for the isolation and purification of total lipids from animal tissues. *J Biol Chem* 1957;**1**:497–509.
22. Allain CC, Poon LS, Chan CS *et al*. Enzymatic determination of total serum cholesterol. *Clin Chem* 1974;**4**:470–5.
23. Kriketos AD, Furler SM, Gan SK *et al*. Multiple indexes of lipid availability are independently related to whole body insulin action in healthy humans. *J Clin Endocrinol Metab* 2003;**2**:793–8.
24. Hewitson TD, Darby IA. *Histology Protocols*. New York, USA: Humana Press, 2010.
25. Cardiff RD, Miller CH, Munn RJ. Manual hematoxylin and eosin staining of mouse tissue sections. *Cold Spring Harb Protoc* 2014;**6**:pdb-rot073411.
26. Trott O, Olson AJ. Auto Dock Vina: improving the speed and accuracy of docking with a new scoring function, efficient optimization, and multithreading. *J Comput Chem* 2010;**2**:455–61.
27. Ishizuka M, Ohtsuka E, Inoue A *et al*. Abnormal spermatogenesis and male infertility in testicular zinc finger protein Zfp318-knockout mice. *Dev Growth Differ* 2016;**7**: 600–8.
28. Skinner MK, Griswold MD. Sertoli cells synthesize and secrete transferrin-like protein. *J Biol Chem* 1980;**20**: 9523–5.
29. Maqdasy S, Baptissart M, Vega A *et al*. Cholesterol and male fertility: what about orphans and adopted? *Mol Cell Endocrinol* 2013;**1-2**:30–46.
30. Sèdes L, Thirouard L, Maqdasy S *et al*. Cholesterol: a gatekeeper of male fertility? *Front Endocrinol* 2018;**9**:369.
31. Azzarito C, Boiardi L, Vergoni W *et al*. Testicular function in hypercholesterolemic male patients during prolonged simvastatin treatment. *Horm Metab Res* 1996;**4**:193–8.
32. Ramirez-Torres MA, Carrera A, Zambrana M. High incidence of hyperestrogenemia and dyslipidemia in a group of infertile men. *Ginecol Obstet Mex* 2000;**68**:224.
33. Liu CY, Chou YC, Lin SH *et al*. Serum lipid profiles are associated with semen quality. *Asian J Androl* 2017;**6**:633.

34. Lo EM, Rodriguez KM, Pastuszak AW, Khera M. Alternatives to testosterone therapy: a review. *Sex Med Rev* 2018;**1**:106–13.
35. Kim N, Nakamura H, Masaki H *et al*. Effect of lipid metabolism on male fertility. *Biochem Biophys Res Communique* 2017;**3**:686–92.
36. Eacker SM, Agrawal N, Qian K *et al*. Hormonal regulation of testicular steroid and cholesterol homeostasis. *Mol Endocrinol* 2008;**3**:623–35.
37. Cadenas E, Sies H. Oxidative stress: excited oxygen species and enzyme activity. *Adv Enzyme Regul* 1985;**23**:217–37.
38. Peltola V, Mäntylä E, Huhtaniemi I, Ahotupa M. Lipid peroxidation and antioxidant enzyme activities in the rat testis after cigarette smoke inhalation or administration of polychlorinated biphenyls or polychlorinated naphthalenes. *J Androl* 1994;**4**:353–61.
39. Elroy-Stein O, Bernstein Y, Groner Y. Overproduction of human Cu/Zn-superoxide dismutase in transfected cells: extenuation of paraquat-mediated cytotoxicity and enhancement of lipid peroxidation. *EMBO J* 1986;**3**:615–22.
40. Allery JP, Telmon N, Blanc A *et al*. Rapid detection of sperm: comparison of two methods. *J Forensic Leg Med* 2003;**1**:5–7.
41. Gadekar GP, Baile VV. Histochemical distribution of acid phosphatase in the tissues of Indian Major carp, Labeorohita (ham). *Mater Today* 2018;**10**:22317–27.
42. Vanha-Perttula T. Spermatogenesis and hydrolytic enzymes—A review. *Ann Biol Anim Biochim Biophys* 1978;**18**: 633–44.
43. Najaran H, Bafrani HH, Rashtbari H *et al*. Evaluation of the serum sex hormones levels and alkaline phosphatase activity in rats' testis after administering of berberine in experimental varicocele. *Orient Pharm Exp Med* 2019;**2**:157–65.
44. Rehman AA. Effect of gamma radiation on alkaline phosphatase enzyme in Swiss albino mice. *Asian J Agric Biol* 2016;**1**:36–8.
45. Zirkin BR, Ewing LL, Kromann N, Cochran RC. Testosterone secretion by rat, rabbit, Guinea pig, dog, and hamster testes perfused in vitro: correlation with ley dig cell ultrastructure. *Endocrinology* 1980;**6**:1867–74.
46. Nwonuma CO, Favours GO, Rotimi DE *et al*. Comparative modulatory assessment of the sperm quality and testicular function by solvent fractions of the cannabis extract in rats. *Pharmacogn* 2021; In press.